Investigation of the Equatorial Undercurrent on the eastern side of the Galapagos Islands

Xyrone Ocampo
University of Washington
School of Oceanography
Box 357940
Seattle, Washington 98195-7940

05 March 2006

Non-Technical Summary

My project is about finding and describing a subsurface water current running parallel to and along the Equator in the Pacific Ocean. The Equatorial Undercurrent, or EUC, flows eastward throughout most of the Pacific Basin and acts as a conduit for water mass conservation in the equatorial region. The Galapagos Islands sit atop a platform located in the middle of the EUC path, which acts as a barrier to the EUC flow. The water dynamics east of this platform are still not completely understood. To try to better define the flow, I gathered velocity and hydrographic data during a student field cruise in January 2006. I used an Acoustic Doppler Current Profiler mounted on the Research Vessel Thomas G. Thompson to gather the velocity components of the EUC on the eastern side of the Galapagos platform. In addition, temperature and salinity profiles were gathered using a conductivity, temperature, and depth instrument and two Iridium floats. Results show that an eastward subsurface flow was flowing north of the Galapagos platform and present on the eastern side. The mean temperature and salinity of the EUC east of the Galapagos Islands was 15.1±0.4ºC and 34.98±0.01 practical salinity units, respectively, at a core depth of 67 m.

Acknowledgments

I would like to thank all of the people who have helped me in this project. I would first like to thank my Physical Oceanography advisor Professor Seelye Martin for providing me with the greatest guidance throughout my entire senior project. I would like to thank all parties involved in funding the 2006 Galapagos Islands undergraduate field cruise: The State of Washington for providing the Research Vessel Thomas G. Thompson; the University of Washington and the College of Oceanography for subsidizing the trip to Ecuador; and Tracie Watkins for providing assistance in the trip logistics. I would like to thank the ship's crew of the Thomas G. Thompson for providing a safe journey at sea and being flexible to accommodate the TN-189 leg two logistics. I would like to thank all whom have helped in processing my data: Robert Drucker for creating a wonderful MATLAB program; Ecuadorian Scientist Nathalia Tirado for processing my salinity data and teaching me Spanish; and Aaron Morello for assisting me with the Portasal. I would like to thank Professor Oscar Vilches and Subramanian Ramachandran from the UW School of Physics for working around my schedule to accommodate my Physics class. I would like to thank Dana Swift and Stephen Riser for allowing me to use two of their Iridium floats. I would like to thank Dr. William Kessler of NOAA for helping me analyze my data. I would like to thank my Physical Oceanography classmate Kevin Odle for allowing me to use his data from TN-189 leg one. I would like to thank Llyd Wells for the timely and meticulous critiques of each of my drafts. Finally, I would like to thank the other OCEAN 444 professors who have contributed so much in making my project a success: Professor Gabrielle Rocap for all the constructive feedback; Professor Mark Holmes for all the cruise logistics; and Professor Roy Carpenter for his vision to make the Galapagos Senior trip a reality.

Abstract

Hydrographic data and Acoustic Doppler Current Profiler (ADCP) measurements were taken at 089ºW from 2ºS to 0.5ºN to capture the signature of the Equatorial Undercurrent (EUC) east of the Galapagos Islands. The EUC, a subsurface eastward flowing current located along the Equator, is well-studied west of the Galapagos Islands. However, the nature of the current east of the Galapagos Islands is not well understood. This study was designed to determine the current dynamics of the EUC east of the Galapagos during the second leg of a two-leg student field cruise conducted on 20-28 January 2006 aboard the Research Vessel (R/V) Thomas G. Thompson, and compare the behavior to previous hydrographic and velocity data. Hydrographic and velocity data collected from leg one of the student cruise on 12-20 January 2006 at 092ºW are also used to determine the location of the EUC west of the Galapagos Islands. The core of the EUC was detected at ~0.1ºN along 092ºW and flowing north of the Galapagos Islands, with a mean depth of 73 m, mean temperature of 15.3±0.9ºC, and salinity of 35.01±0.05 psu. The EUC shallowed to 67 m with a 15.1±0.4°C mean temperature and a salinity of 34.98±0.01 psu at 089°W.

Introduction

The Galapagos Islands sit atop a platform that provides a topographic barrier impeding the South Equatorial Current (SEC) and the Equatorial Undercurrent along the Equator (Fig. 1; Eden and Timmerman 2004). The SEC is a westward-flowing surface current driven by the trade winds. These trade winds cause water to pile up in the western side of the Pacific Basin, leading to a zonal pressure gradient within the Equatorial Pacific. The water mass imbalance is rectified by an eastward subsurface return flow called the EUC (Christensen 1971; Blanke and Raynaud 1997).

The presence of the Galapagos Islands as a barrier in this region results in complex flow patterns of the EUC (Eden and Timmerman 2004). To the west of the Galapagos Islands, the mean flow of the Equatorial Undercurrent is zonal, i.e. a function of latitude alone (Kessler 2005). There, the EUC can extend from 2ºS to 2ºN, at a core depth of 50-275 m (Steger et al. 1998). According to Lukas (1986), the signature of the EUC included a 14.86±0.23ºC mean temperature at 100 m and a large salinity maximum of 35.01±0.02 psu observed at 092ºW. The inferred transport was estimated at 30-40 Sverdrups (Blanke and Raynaud 1997) with a peak velocity of about 1 m s^{-1} (Steger et al. 1998).

To the east of the Galapagos Islands, the Equatorial Undercurrent may recur, but the proximity of the South American continent becomes the dominant factor, producing strong meridional winds and zonal variations of forcing and properties (Kessler 2005). Lukas (1986) gave representative mean values of 14.65±0.22ºC water at 100 m with a high salinity maximum of 35.00±0.02 psu at 088ºW. Knauss, as mentioned in Steger et al. (1998), observed the core of the EUC deepening (160-250 m) with respect to 092ºW and a reduced velocity (0.1-0.25 m s^{-1}) at 089ºW. The flow spreads over a larger meridional distance, with the core sometimes displaced

south or north of the Galapagos Islands (Christensen 1971). Observations from February 1966 (Christensen 1971) and in October and December 1971 by Pak and Zanaveld, as mentioned by Steger et al. (1998), showed the EUC flowing to the north and weak and irregular EUC flow, if any, to the south. This variation in displacement is not understood well enough to determine whether it is due to seasonal variability or unstable flow conditions (Lukas 1986; Eden and Timmerman 2004).

Thus, the true flow pattern of the EUC around the Galapagos has not been fully determined. Eden and Timmerman (2004) argue that the Galapagos Islands shield the EUC from the coast of South America, with only a small appendage of the current reaching the coast during the boreal winter. Christensen (1971) states that mechanisms involved in the diminution of the eastward flow are unclear and that the EUC abandons its course some distance from South America. Lukas (1986) does not define the end of the EUC, but instead says that the source waters of the Peru-Chile Undercurrent, an eastward current that flows adjacent to the South American continent, is probably from the EUC, and that the EUC extends southward from the Equator to the continent.

These uncertainties led me to examine the nature of the EUC east of the Galapagos Islands. Since previous observations have shown eastward flow to the north of the islands during the northern hemisphere winter months, I expected the majority of the flow of the EUC to be at the northern boundary of the platform. Given the relative size of the Galapagos platform when compared to the EUC dynamics, I anticipated that the platform would play a role similar to a rock in the river in the conduit that runs along the Equator. That is, water that flowed around the rock would be diverted but continue around the rock. If there were an eastward flow east of the

Galapagos platform, then I would expect the flow to have the same properties as the EUC west of the Galapagos Islands.

I collected current profiles and hydrographic data east of the Galapagos platform to determine current magnitudes and directions, temperature, salinity, and water density characteristics. The main location of analysis was along a meridional transect at 089ºW longitude, which I have compared with previous work by Steger et al. (1998) in the same location. I also used ADCP data collected by Odle (2006) at 092ºW to locate where the EUC was coming from in the west and to compare to my data.

Methods

Near continuous ADCP profiles and hydrographic conductivity, temperature, and depth (CTD) data from six stations were collected from 20-28 January 2006, during the second leg of a joint scientific cruise with University of Washington students and Ecuadorian scientists aboard the R/V Thomas G. Thompson. A meridional transect along 089ºW (Fig. 2) began at station XO1, located at 2ºS, and ended at XO6, located at 0.5ºN. Two Iridium floats were also deployed to give a spatiotemporal picture of the water surrounding the Galapagos platform.

A hull-mounted 75 kHz RDI (RD Instruments 1996) ADCP was used to monitor the east (u) and north (v) velocity components. These velocity components were averaged in 1 min ensembles in 8 m thick bins. 50 bins were used to record to 400 m depth with the bottom boundary of bin 1 set at 28 m depth. Data were collected using WinADCP software. Calibration was performed by Seelye Martin and Rob Hagg on 26 January 2006, prior to an 089ºW meridional transect, to correct an 0.85º offset between the ship navigation and the ADCP

orientation (Martin, S., pers. comm.). During each ADCP profile, the ship maintained a 10-knot speed of advance for data consistency.

Hydrographic sampling was constrained to depths of 400 m, sufficient to observe characteristics through the entire EUC. Salinity, temperature, and density data were collected using a 24-Niskin bottle Seabird CTD rosette. Six CTD casts were taken along the transect at half-degree intervals, with the exception of the 1ºS latitude, where the bottom shoals to less than 400 m. The station XO3 was therefore moved from 1ºS to 0.93ºS.

Seawater samples were collected at stations XO1 and XO6 to ensure proper calibration of the Seabird conductivity sensor. Because the shipboard salinometer was not functioning, Nathalia Tirado, a scientist from the Darwin Research Station, analyzed the seawater salinity sampled from station XO1 at 0 m, 20 m, 100 m, 200 m, and 300 m, upon return to Isla Santa Cruz (Table 1). A second set of seawater samples were brought back to the University of Washington for salinity analysis.

After my return to Seattle, I analyzed the seawater salinity sampled in triplicate from station XO6 at 0 m, 100 m, 200 m, 300 m, and 350 m (Table 1) using a Guildline Portable Salinometer (Portasal Model 8410). The sample bottles were stored at least 24-hours in the same room as the Portasal to allow the temperature of the samples to equilibrate with the salinometer. The Portasal, accurate to within ±0.003 psu, was first calibrated to a seawater standard from Ocean Services, Inc. Each of the seawater samples were then run through the conductivity cell and flushed three times. The salinity measurements were then recorded when two consecutive readings were within ±0.001 psu.

Two Iridium floats, operated by Dana Swift and Stephen Riser at the University of Washington, were deployed at stations XO1 and XO6 to drift at 100 m. These floats were used to

gather hydrographic data (in situ temperature, salinity, and density) in addition to drifting with the 100 m current. These pre-programmed floats followed a two-day cycling time, consisting of the floats drifting for a two-day period, dropping to 1000 m and floating up to the surface to take a CTD profile at the end of the cycle. The float deployed at XO1 had ID# 0020 and the float at XO6 had ID#5044. Float 0020 can be monitored at http://runt.ocean.washington.edu/argo/homographs/TP/TP.html. Float 5044 was lost around 6 February 2006.

MATLAB, WinADCP, and Microsoft Excel software were used to analyze the velocity and hydrographic data. MATLAB m-files were created by Robert Drucker from the University of Washington to provide velocity vectors from each of the ADCP profiles. WinADCP was used as a graphical user interface to represent the *u* and *v* velocity components in a color scale. Temperature, salinity, and density profiles were analyzed using Microsoft Excel.

Results

The results are presented as a series of ADCP velocity components, hydrographic properties along the 089ºW transect via CTD data, and hydrographic properties from the two Iridium floats.

Velocity components

I used the information from bins 1, 3, 5, 7 and 10 from all my ADCP data collected during the cruise, which represent the current velocities at 28 m, 44 m, 60 m, 76 m and 100 m, respectively. This included an ADCP profile recorded on the way back to Isla Santa Cruz in addition to the 089ºW transect. I also used Odle (2006) ADCP data collected at the 092°W

longitude, from 1.5°S to 0.6°N. I limited the interpretation to the upper 100 m because eastward velocities at both 089ºW and 092ºW were greatest at this depth range (Fig. 3). However, eastward velocities were still present below 100 m, but the definition of the eastward flow appeared intermittent. The only caveat is that the ADCP data west of 090°W were collected prior to the calibration by Martin and Hagg on 26 January 2006. With the ADCP profiles collected at 10 knots, zonal errors were as much as 73 mm s^{-1}; only trivial (0.5 mm s^{-1}) meridional errors were noted (Martin, S., pers. comm.). General trends were mentioned from each depth investigated.

The 28 m depth bin was the shallowest bin observed. The flow at this depth showed no signs of the EUC from the west (Fig. 4A). The rest of the ADCP profiles showed a northward flow around 300 mm s^{-1} at both meridional transects, but the trend shifted from a northwestern flow to a relatively stronger northeastern flow north of 1°S at the 089°W transect. The ADCP profile northwest of the 089ºW transect included a southwestern flow of less than 300 mm s^{-1}.

The EUC appeared at the 44 m depth bin profile (Fig. 4B). The ADCP profiles showed large directional changes to the west of Isla Isabela and more pronounced zonal directions east of the Galapagos platform. At the 092°W transect, divergence was seen centered at 0.75ºS as the direction south of this had a southwestern flow and north of this had a northeastern flow, with mean flow near 300 mm s^{-1}. North of the Equator, the flow was directly eastward at ~500 mm s^{-1}. The velocity directly north of Isla Isabela also showed a large shift in direction, from a strong northwestern flow to a less than 200 mm s^{-1} eastward flow. At the 089°W transect, the direction and magnitude north of 1°S was east southeastward at 200 mm s^{-1} and west-northwestward at 200 mm s^{-1} south of 1°S. The 60 m depth (Fig. 4C) is similar to the 44 m profile, but just

emphasizes the velocity signature located northwest of Isla Isabela. Peak eastward velocities were over 600 mm s^{-1} and a strengthening of the eastward velocity vectors were present north of 0.75°S at the 092°W transect.

At 76 m (Fig. 4D), the EUC persisted with depth, and meridional broadening eastward flow northwest of Isla Isabela was seen, with the average velocities in this region over 600 mm s^{-1}. Peak velocities at 092ºW were highest at this depth range, reaching as high as ~900 mm s^{-1} (Fig. 3A) at 0.1ºN. Along the 092°W transect south of 0.75ºS, the velocities were well to the south at magnitudes of 150 mm s^{-1}. The flow north of the Equator at the 089°W transect has developed into a south-southeastern flow, also seen on the ADCP profile northwest of the transect.

The 100 m depth profile (Fig. 4E) showed minor changes west of the Galapagos Islands, but a noticeable change in the east. At the 092°W transect, the velocities south of 0.75°S changed to 100 mm s^{-1} to the east. Velocities north of this latitude reduced to 450 mm s^{-1}, but still maintained its eastward direction. At 089°W, the water appeared to diverge near the 1°S latitude, with a southern flow of 300 mm s^{-1} to the north and a westward flow of 300 mm s^{-1} to the south. Shallow topography was present at this location (Fig. 3C).

East-West Component at 089°W

From 2°S to 1°S, there is an overall westward flow, with the fastest velocities along the 100 m and 300 m depths (Fig. 5A). The mean velocity is 250 mm s^{-1} with peak velocities around 600 mm s^{-1} around 1°S near the surface. Ambiguous returns were noticed around the shoal areas at 200-400m depth at 1°S. This region coincided with the divergence noticed in Fig. 4E.

The first observation of an eastward tongue was at 1°S at 36 m. This eastward flow becomes more prominent north of this boundary, with eastward depths as much as 50 m at 0.8°S and with a peak eastward velocity of 630 mm s^{-1} located near the same latitude. This eastward flow begins to shallow as the transect approaches 0.5°S, and begins to increase in thickness to 84 m depth at the lower boundary between 0.5°S and the equator. This broadened band has a relatively slower mid-depth eastward velocity, having mean velocities greater than 500 mm s^{-1} near the surface, 250 mm s^{-1} at 52 m, and 300 mm s^{-1} at 76 m. A narrow band about 10 m thick with a core depth of 100 m becomes distinguishable at 0.2ºN, and continues northward past the 0.5ºN boundary of the 089ºW transect. Peak velocities in this eastward band are near 300 mm s^{-1}.

North-South Component at 089°W

From 2ºS to 1ºS, the net flux is northward at velocities varying from 0-100 mm s^{-1} in the upper 300 m, but the flow from 300-400 m has a net flow to the south, around 100 mm s^{-1} (Fig. 5B). North of the shoaling at 1ºS, a relatively strong southern flow is present in the upper 200 m, starting near 50 mm s^{-1} right at the shoaling to 250 mm s^{-1} around 0.75ºS. Peak southward velocities in this region reach 400 mm s^{-1}. The mean velocity in the upper 200 m reaches 300 mm s^{-1} between 0.5ºS through 0.5ºN, but from 200-400 m the net flow varies from 0-50 mm s^{-1} northward.

CTD Data

The CTD data collected along the 089°W transect were broken down into the temperature, salinity, and density profiles. To compare the water spatially east of the Galapagos Islands, the profiles from the six stations were averaged at each depth and individual stations

were compared to the mean at each depth (Fig. 6). These profiles were used to determine the general trends of temperature, salinity, and density along the 089ºW transect.

Temperature differences were greatest in the upper 140 m. Below this depth, the temperature decreased uniformly from 13.9±0.1°C at 140 m to 9.7±0.2°C at 400 m. Above 140 m, the largest change occurred at 10-40 m, with peak changes at 20 m. Here, the mean was 20.1±2.3°C. Surface temperatures varied slightly throughout this transect, from 24.8ºC at station XO2 to 26.0ºC at station XO4. The mean surface temperature was 25.5 ±0.5°C at the 089°W transect. The general trend at this transect was warmer waters at the southern three stations and cooler waters at the northern stations at 10-40 m, but the surface waters had the opposite trend (Fig. 6A). The thermocline south of 0.93ºS ranged from 17-36 m, but north of this latitude the thermocline shallowed to 7-20 m. Below 40 m, the deviation from the mean at each station was variable.

The salinity properties in this region parallel with the temperature properties (Fig. 6B). The depths where greatest changes occurred were from 15-40 m, with the peak change in salinity of 34.58±0.31 psu occurring at 25 m. Below 140 m had minimal changes, with the salinity maximum of 35.00±0.02 psu occurring from 66-103 m. The surface salinity freshened northward along the transect, from a maximum of 34.25 psu at XO1 to 33.59 psu at XO6. Like the thermocline, the halocline hovered around 30 m, at the southern three stations, but the northern three stations had shallower haloclines between 8-17 m. The general salinity trend showed fresher surface waters in the north, with four of the six stations below the mean. At the 15-40 m depths, the salinity signature was opposite that of the surface waters, with the most saline waters in the northern three stations and a relatively fresh tongue to the south.

Since density is a function of salinity and temperature, especially at the surface, the profile follows a similar shape to the previous profiles (Fig. 6C). Surface waters north of the 1°S barrier were less dense, but were denser in the 15-40 m depths. Mean surface waters were σ = 22.4±0.3 and the greatest deviation was σ = 24.3±0.8 at 20 m.

The seawater samples analyzed from XO1 and XO6 used to calibrate the conductivity instrument on the CTD showed different results in magnitude of standard deviation (Table 1). The data processed by Nathalia Tirado shows a standard deviation of ±.05, whereas the data I processed was ±.01.

The surface waters gradually became less dense from 2ºS to 1º30'N, from σ=22.8 at XO1 to σ=22.0 at XO6. The pycnocline mirrored the temperature and salinity profiles, which had a mean depth of ~30 m at the southern three stations, but a shallower 8-20 m depth at the northern three stations.

Iridium float data

Float 0020, deployed at 2ºS and 100 m, traveled west-southwestward (Fig. 7), indicating a dominant westward flow. It continues currently along that trajectory. At its programmed 100 m depth, it has measured characteristic water temperatures of 14-15ºC and a salinity of ~35 psu, with the density at ~26.1. Float 5044, deployed at 0.5ºN, traveled south southeastward, measuring a ~14ºC temperature, salinity slightly lower than 35 psu, and a density at ~25.9 at 100 m.

Interannual variability

It is important to understand the interannual variability in this region because the El Niño phenomenon affects the water properties (Steger et al. 1998). The latest information about the El Nino Southern Oscillation (ENSO) phase showed SST anomalies varying between 0.5 to -1.5ºC in the region east of the Galapagos. The equatorial regions west of the Galapagos show slightly cooler SSTs (less than -1ºC), but the ENSO phase is still above the threshold to consider it as weak La Nina conditions. The Southern Oscillation Index (SOI) was at -0.2 (Climatic Data Center 2006).

Discussion

In my attempt to find the EUC east of the Galapagos Islands, I first looked at the zonal velocity and hydrographic data gathered from Odle (2006) at 092ºW. My purpose was to understand the hydrographic characteristics of the EUC, then search for the same characteristics to the east of the islands. I assumed the region with the highest zonal velocity at 092ºW was the core of the EUC (Fig. 3A), which appeared to be between 0.5ºS to ~0.5ºN with average *u* velocities greater than 500 mm s^{-1} (Fig. 4B-E) and peak velocities (~900 mm s^{-1}) located at 0.1ºN (Fig. 4D). These velocity ranges were consistent with velocity data presented in Steger et al. (1998). The core depth was roughly 73 m, which I defined as the center depth of the strong flow (>500 mm s^{-1}), located between 45-100 m at the equator. The closest CTD station to 0.1ºN, the core of the EUC, was located at the Equator. I found the temperature, salinity, and density of the core to be 15.3±0.9ºC, 35.01±0.05 psu, and σ = 25.92±0.16, respectively (Fig. 8A-C). The temperature at 100 m and salinity maximum (~50-60 m) at the Equator were 14.31ºC and 35.07 psu, respectively. These values differed slightly from the Lukas (1986) values of 14.86±0.23ºC at

100 m and 35.01±0.02 at the salinity maximum, indicating a cooler, saltier EUC I observed compared to the historical representative mean values. This may be due to the slight La Niña effect represented by the -0.2 SOI (Climatic Data Center 2006).

Water currents travel between isopycnals, because it takes energy to penetrate through surfaces of different densities. This understanding allowed me to define the density range of σ = 25.92±0.16 within which the EUC flowed. I assumed that the EUC should be at the same density range at the 089ºW transect, which was not necessarily at the same depth as at 092ºW. I chose 0.5ºS (XO4) as the CTD station within the EUC east of the Galapagos Islands because it was located in the center of the strongest zonal flow, with average velocities near 300 mm s^{-1}. Although peak velocities (~630 mm s^{-1}) occurred at 0.8ºS around 36 m, hydrographic data was not available at this location. At 089ºW, density values similar to the core of the EUC at 092ºW were σ = 25.94±0.10, found from ~48-86 m, with a mean depth of 67 m (Fig. 8D-F). In this case, I used the term mean depth to represent the average EUC flow at 089ºW because I could not distinguish a pronounced core at this transect. The mean temperature and salinity at 0.5ºS were 15.1±0.4ºC and 34.98±0.01 psu, respectively. These values were slightly cooler and fresher than the EUC flow from 092ºW, but within the standard deviation of the 092ºW values. This may have been due to the influence of a cooler tongue of water from the north (Fig. 5B), which may explain the strong southeastern flow at ~60-100 m (Fig. 4C-E). At the most northern station (XO6), the tongue was a relatively cooler (Fig. 6A), denser water mass (Fig. 6C), but similar in salinity (Fig. 6B) to the water observed at XO4. The water temperature at 100 m was 14.3ºC with a salinity maximum of 35.05 psu at 76 m, which was again slightly cooler but saltier than that found in Lukas (1986) at 088ºW and at the Equator.

The two Iridium floats deployed at the boundaries of the 089ºW transect were used to give a spatiotemporal view of the water at 100 m (Fig. 7). They were pre-programmed to cycle every two days, where one of the Iridium floats (0020) followed the SEC, while the other flowed with the EUC (5044). The flow trajectories observed were consistent with the velocity vectors observed at 100 m along 089ºW (Fig. 4E). After 6 February 2006, the float (5044) deployed from station XO6 may have crashed into the shoaling located at ~1ºS.

To compare the EUC with its surrounding waters at depths similar to EUC flow, I observed the temperature and salinity of waters outside the core of the EUC at both 092ºW and 089ºW, from CTD stations at 1.5ºS (Fig. 8). I chose this station to observe non-EUC water because zonal flow was generally westward at this latitude (Fig. 4A-D), with no detection of eastward flow at 089ºW (Fig. 5A).

At 092ºW, surface temperatures were warmer at 1.5ºS than at the equator, but colder at depths of 45-100 m (Fig. 8A). This may mean that since the thermocline gradient was less at the location of the EUC with respect to the surrounding water, vertical mixing may have been present at the Equator. This agrees with the canonical description of upwelling occurring west of the Galapagos Islands. Both stations had similar salinity maximums (~35.07 psu) at 50-60 m (Fig. 8B), so the overall density (Fig. 8C) was a function of temperature at these locations.

At 089ºW, surface temperatures were cooler at 1.5ºS than at 0.5ºS (Fig. 8D). The temperature below the observed core depth at 67 m was slightly cooler at the EUC station with respect to the non-EUC station. The greater temperature gradient located at 0.5ºS may mean that upwelling was not common at this longitude due to a relatively steeper, shallower thermocline.

This thermocline, coupled with the relatively shallow halocline above 20 m (Fig. 8E), indicates a shallow pycnocline above the EUC waters (Fig. 8F).

Steger et al. (1998) observed the core of the EUC at 092ºW centered along 0.5ºS at 70 m (Fig. 3B). The core during the January 2006 cruise was centered along ~0.1ºN at 73 m, which was a shift of over half a degree northward, but similar in depth. This observation indicated that the EUC flow in January 2006 had greater velocities concentrated to the north (Fig. 3A). The EUC diverged into two legs in November 1993 (Steger et al. 1998), but due to the EUC displacement north of the Equator in January 2006, the EUC was not observed to flow south of the Galapagos Islands.

EUC flow at 089ºW was observed in November 1993 (Steger et al. 1998) at two locations (Fig. 3D) with reduced speed (~200 mm s^{-1}). The southern core was observed along 1ºS at 50 m, whereas a northern flow was observed at 140 m in the northern hemisphere. Observations in January 2006 indicated a flow was present, though not well-defined, north of 0.93ºS and spread meridionally past observations at 0.5ºN, and flowed in a southeastern direction. This flow is consistent was analogous to my description of the current flowing around the Galapagos platform like a rock in the river. The mean flow of the EUC was ~300 mm s^{-1}, with a mean depth of 67 m. The shoaling at 1ºS appeared to have acted as a barrier to the northern waters during the January 2006 cruise (Fig. 3C), but did not seem to affect the observed convergence in November 1993 (Fig. 3D).

Conclusion

This paper provides evidence from CTD and ADCP profiles that the EUC flows in a weakened form east of the Galapagos Islands. When compared to historical hydrographic and

velocity data, the variability of the EUC was seen during the January 2006 cruise. Understanding the EUC characteristics in the region east of the Galapagos Islands is important because of its effect on equatorial biology. The EUC is an important conduit that not only provides a mass balance in the equatorial Pacific, but also supplies nutrients for the biology. Since the majority of the fauna living among the Galapagos Islands rely heavily upon the sea as a source for food, it is important in understanding which route their food supply comes from. Future studies may include devoting a transect up to 2ºN along 089ºW at this same time of the year to look at water transport study and see if all that is flowing into the west is coming out at the east within the historical parameters (2ºS-2ºN).

References

Blanke, B. and S. Raynaud. 1997. Kinematics of the Pacific Equatorial Undercurrent: An Eularian and Lagrangian approach from GCM results. J. Phys. Ocean. **27**: 1038-1053.

Christensen, N. 1971. Observations of the Cromwell Current near the Galapagos Islands. Deep-Sea Res. Ocean. **18**: 27-33.

Climatic Data Center. 2006. Climate of 2005 El Niño/Southern Oscillation. NOAA website. http://www.ncdc.noaa.gov/oa/climate/research/2005/enso-monitoring.html

Eden, C., and A. Timmerman. 2004. The influence of the Galapagos Islands on tropical temperatures, currents and the generation of tropical instability waves. Geo. Res. Lett. **31**: L15308 1-4.

Kessler, W. 2005. The circulation of the eastern tropical Pacific: A review. Prog. Ocean. **2580**: 1-53.

Lukas, R. 1986. The termination of the Equatorial Undercurrent in the Eastern Pacific. Prog. Oceanog. **16**: 63-90.

Odle, K. 2006. An investigation of the EUC along 92W, from 1.5S to 0.75N recorded during 13-23 January 2006. Unpublished Bachelor's Thesis, University of Washington.

RD Instruments. 1996. Acoustic Doppler Current Profiler-Principles of operation, A practical primer. 2nd ed. RD Instruments.

Steger, J., C. Collins, and P. Chu. 1998. Circulation in the Archipiélago de Colón (Galapagos Islands), November, 1993. Deep-Sea Res. II **45**: 1093-1114.

Table 1. Salinity calibration results. The salinity calibration analysis for water samples at station XO1 was performed by Ecuadorian scientist Nathalia Tirado of the Charles Darwin Research Station in the Galapagos Islands. The salinity calibration analysis for water samples at station XO6 was conducted by Xyrone Ocampo at the University of Washington in Seattle, Washington.

Salinity measurements for water samples taken at XO1

Bottle	Depth (m)	Salinity (psu)	CTD Sal 1	CTD Sal 2	CTD Avg	Diff(CTD-meas)
145	300	35.100	34.799	34.799	34.799	-0.301
146	300	35.100	34.799	34.799	34.799	-0.301
147	300	35.100	34.799	34.799	34.799	-0.301
148	200	35.200	34.952	34.951	34.952	-0.249
149	200	35.200	34.952	34.951	34.952	-0.249
150	200	35.200	34.952	34.951	34.952	-0.249
151	100	35.400	35.046	35.045	35.046	-0.354
152	100	35.400	35.046	35.045	35.046	-0.354
153	100	35.400	35.046	35.045	35.046	-0.354
154	20	34.600	34.247	34.248	34.248	-0.352
155	20	34.600	34.247	34.248	34.248	-0.352
156	20	34.600	34.247	34.248	34.248	-0.352
157	0	34.500	34.264	34.264	34.264	-0.236
158	0	34.500	34.264	34.264	34.264	-0.236
159	0	34.500	34.264	34.264	34.264	-0.236
					Std Dev	0.052

Salinity measurements for water samples taken at XO6

Bottle	Depth (m)	Salinity (psu)	CTD Sal 1	CTD Sal 2	CTD Avg	Diff (CTD-Meas)
1	350	34.752	34.764	34.762	34.763	0.011
2	350	34.752	34.764	34.762	34.763	0.011
3	350	34.750	34.764	34.762	34.763	0.013
4	300	34.803	34.748	34.813	34.781	-0.022
5	300	34.803	34.748	34.813	34.781	-0.022
6	300	34.803	34.748	34.813	34.781	-0.022
7	200	34.921	34.899	34.938	34.919	-0.002
8	200	34.922	34.899	34.938	34.919	-0.003
9	200	34.946	34.899	34.938	34.919	-0.027
10	100	34.964	34.937	34.975	34.956	-0.008
11	100	34.965	34.937	34.975	34.956	-0.009
12	100	34.964	34.937	34.975	34.956	-0.008
13	0	33.583	33.541	33.578	33.560	-0.023
14	0	33.584	33.541	33.578	33.560	-0.025
15	0	33.586	33.541	33.578	33.560	-0.026
					Std Dev	0.014

Figure Legends

Figure 1. A schematic representation of the currents surrounding the Galapagos Islands. The South Equatorial Current flows westward on the surface and around the eastward subsurface Equatorial Undercurrent. Areas in green are locations where the EUC upwells. Photo from unknown author.

Figure 2. This chart shows the R/V Thomas G. Thompson cruise during 20-28 January 2006. The solid line represents the track line of the cruise, where blue denotes the track pertaining to this project and red represents the rest of the cruise. CTD stations XO1-XO6, represented by blue boxes, were used to collect hydrographic data. At stations XO1-XO6, Iridium floats were deployed.

Figure 3. Zonal velocity current profiles from 092ºW (A, C) and 089ºW (B, D) during two separate cruises. (A) and (C) profiles were collected during the 12-28 January 2006 cruise. (A) had a data blank from 0.1ºS to the equator because no ADCP data was available. (B) and (D) profiles were obtained from a cruise on 8-19 November 1993 (Steger et al. 1998). Each panel used the same magnitude scale (in mm s^{-1}) for easier comparison.

Figure 4. Velocity vectors of ADCP profiles taken around the Galapagos from (A) 28 m, (B) 44 m, (C) 60 m, (D) 76 m, and (E) 100 m. Background chart from Chadwick at http://newport.pmel.noaa.gov/~chadwick/galapagos.html.

Figure 5. ADCP velocity representations. (A) East-West component from 2ºS to 0.5ºN. (B) North-South component from 2ºS to 0.5ºN.

Figure 6. Hydrographic data taken from the 089°W transect at six stations, XO1-6. (A) Temperature difference from the mean at each depth, (B) Salinity difference from the mean at each depth, and (C) Density difference from the mean at each depth.

Figure 7. Trajectory profile for float ID 0020 (yellow) and float ID 5044 (blue). The floats were released at stations XO1 and XO6, respectively, and were given a cycle time of 2 days at 100 m. Background chart from Chadwick at http://newport.pmel.noaa.gov/~chadwick/galapagos.html.

Figure 8. Temperature, salinity, and density profiles for (A-C) 092ºW and (D-F) 089ºW. Panels (A-C) show hydrographic data at two stations along the transect, one located within the EUC (Equator) and one located outside of the EUC (1.5ºS). Panels (D-F) show hydrographic data at two stations along the transect similar to Panel (A-C), except the one located within the EUC is at 0.5ºS.

Figure 1.

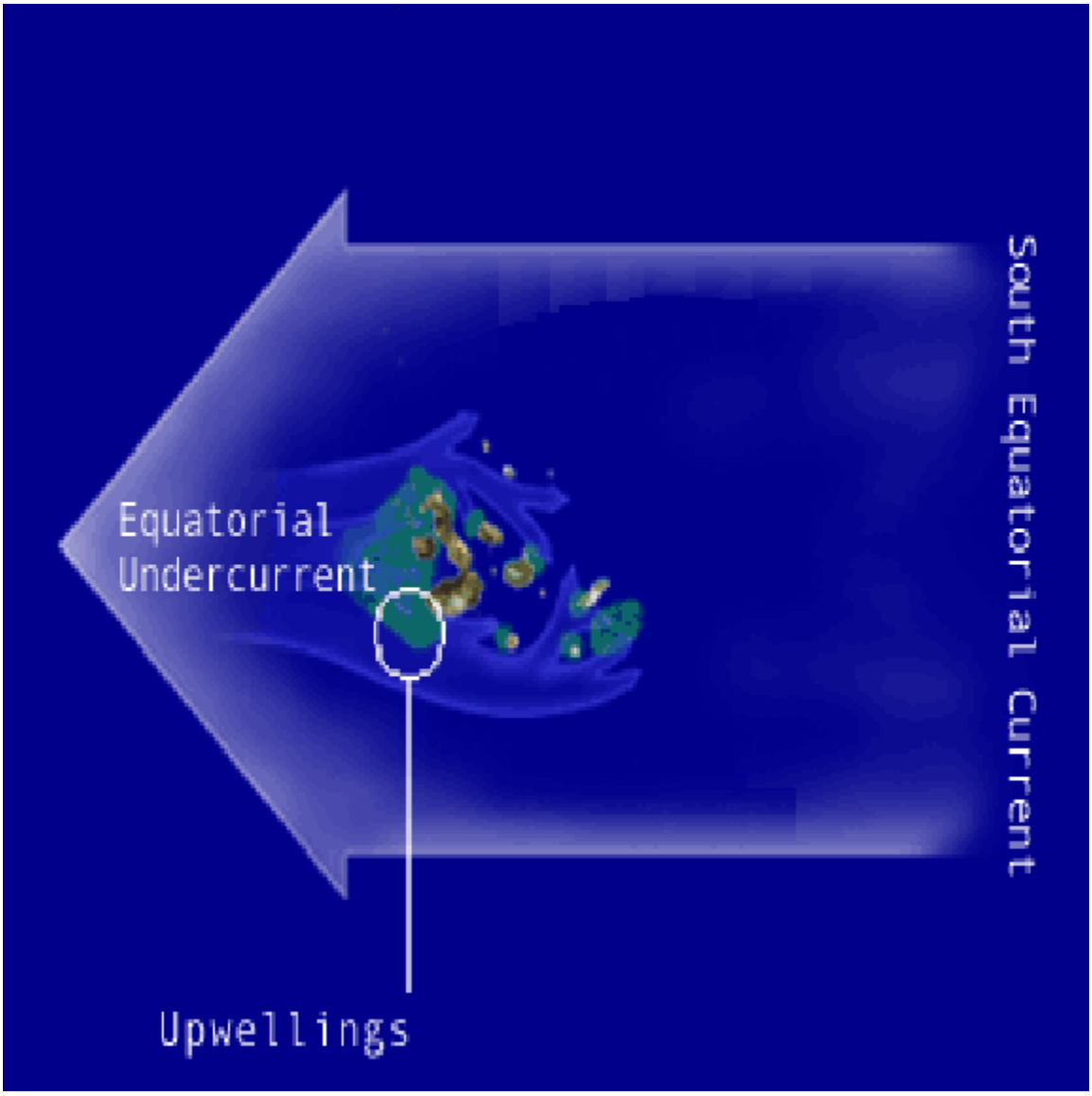
South Equatorial Current
Equatorial
Undercurrent
Upwellings

Figure 2.

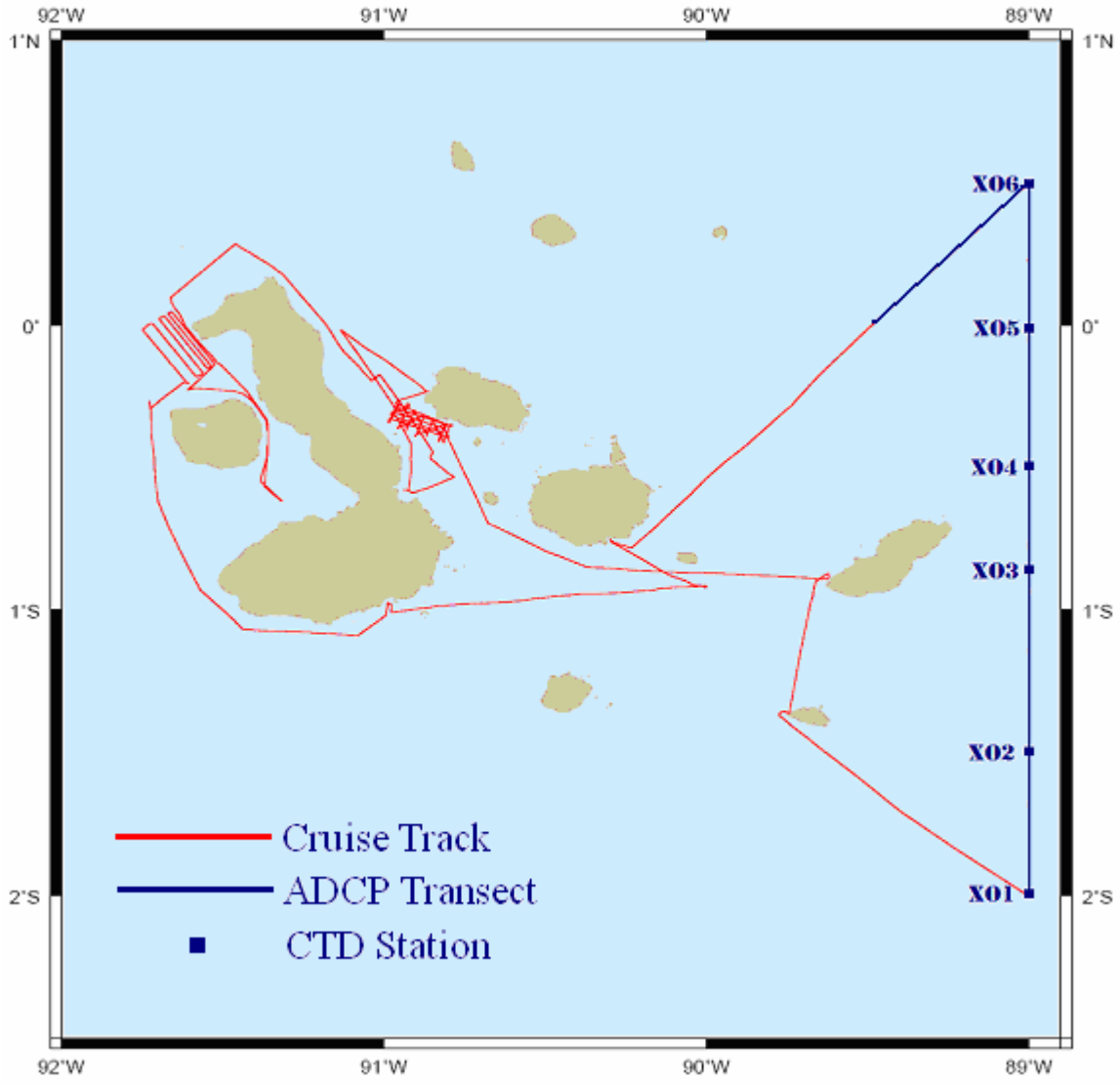
92°W
91°W
90°W
89°W
1°N
0°
1°S
2°S
XO6
XO5
XO4
XO3
XO2
XO1
Cruise Track
ADCP Transect
CTD Station

Figure 3.

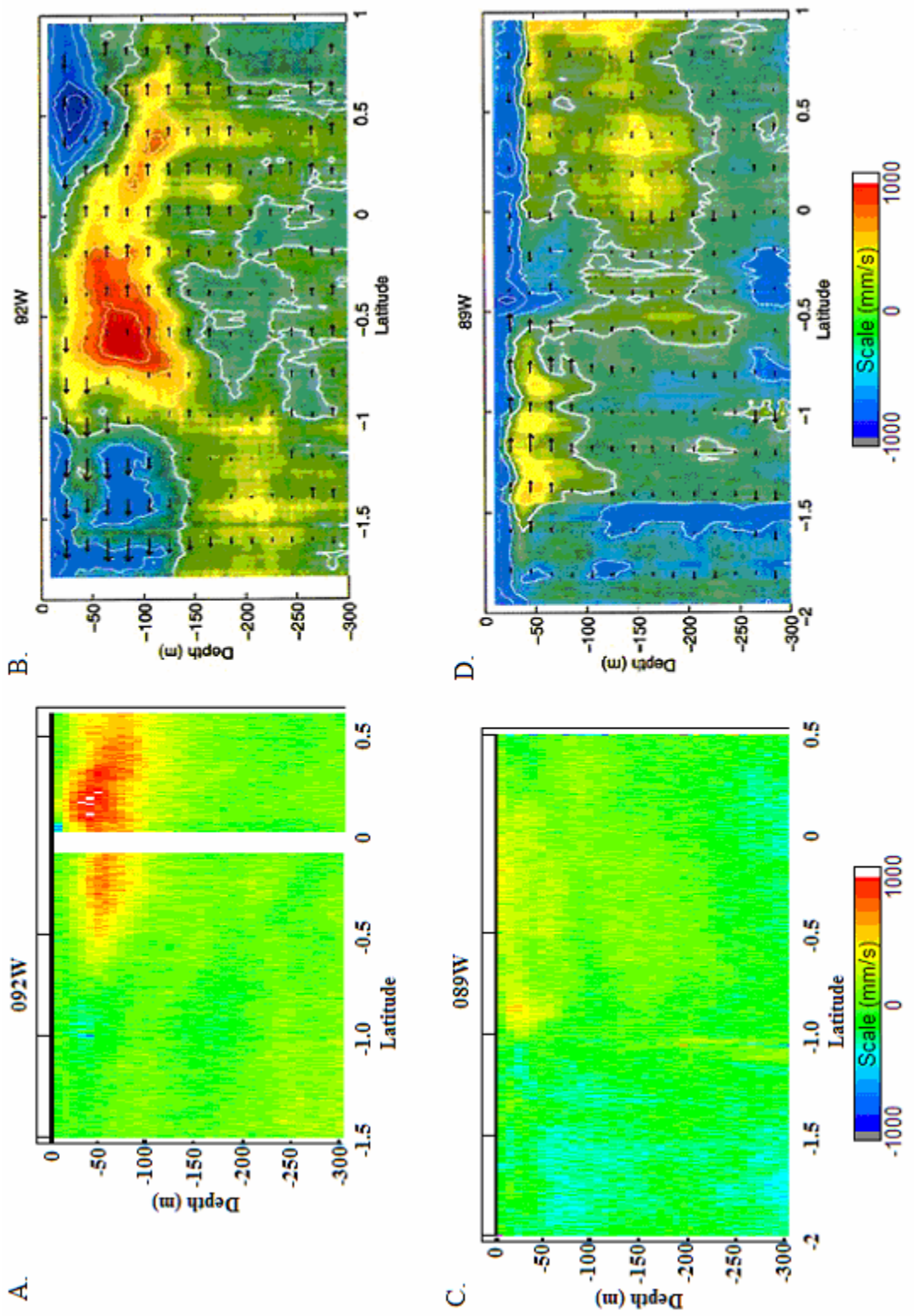
A.
092W
Depth (m)
Latitude
B.
92W
Depth (m)
Latitude
C.
089W
Depth (m)
Latitude
Scale (mm/s)
D.
89W
Depth (m)
Latitude
Scale (mm/s)

Figure 4.

A. Velocity vectors at 28 m.

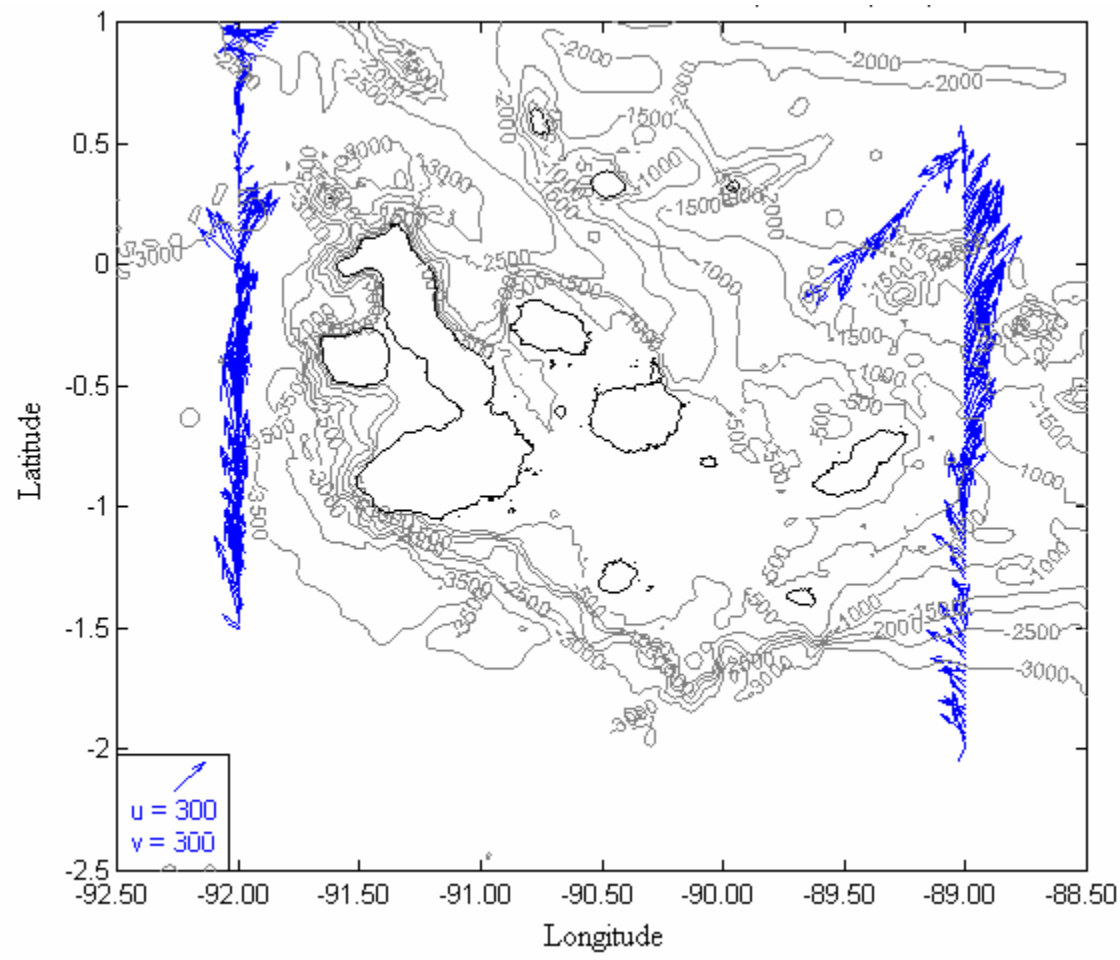

B. Velocity vectors at 44 m.

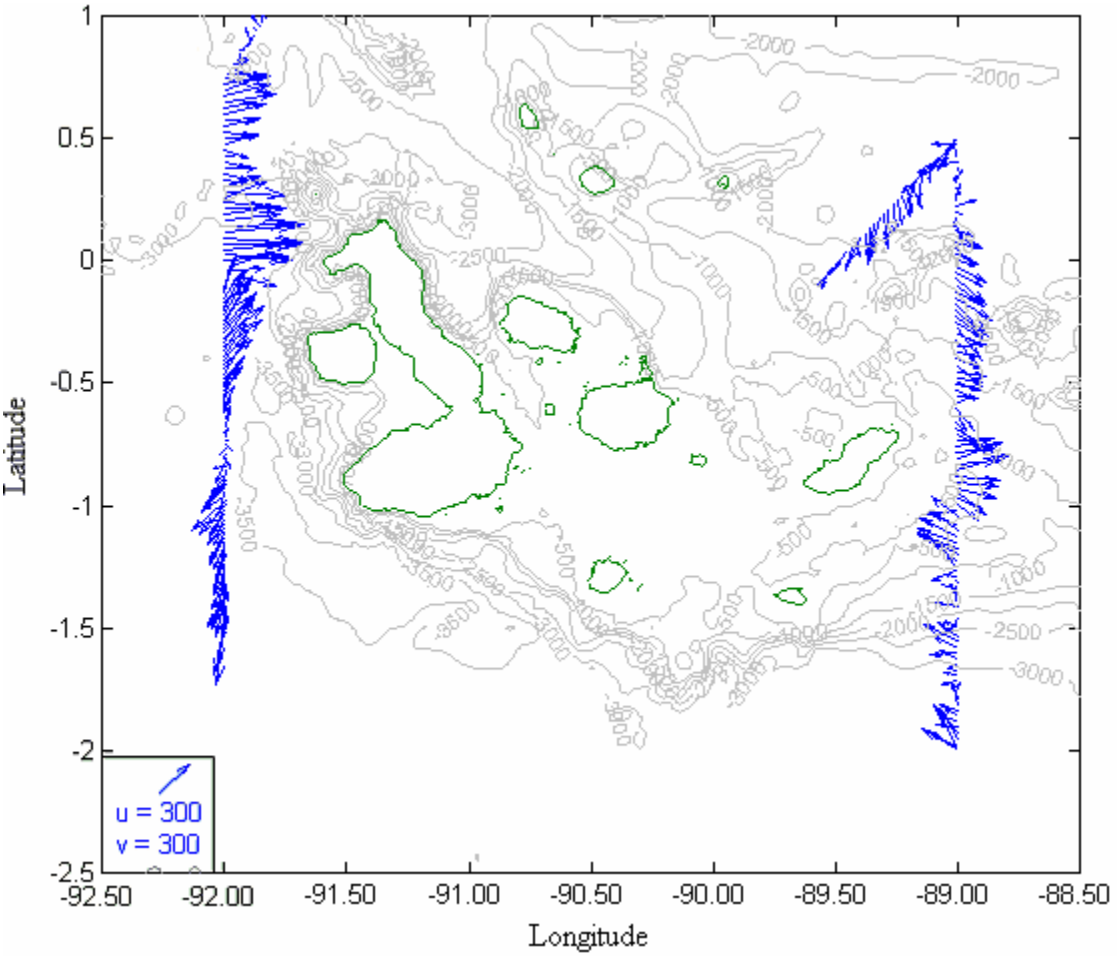

C. Velocity vectors at 60 m.

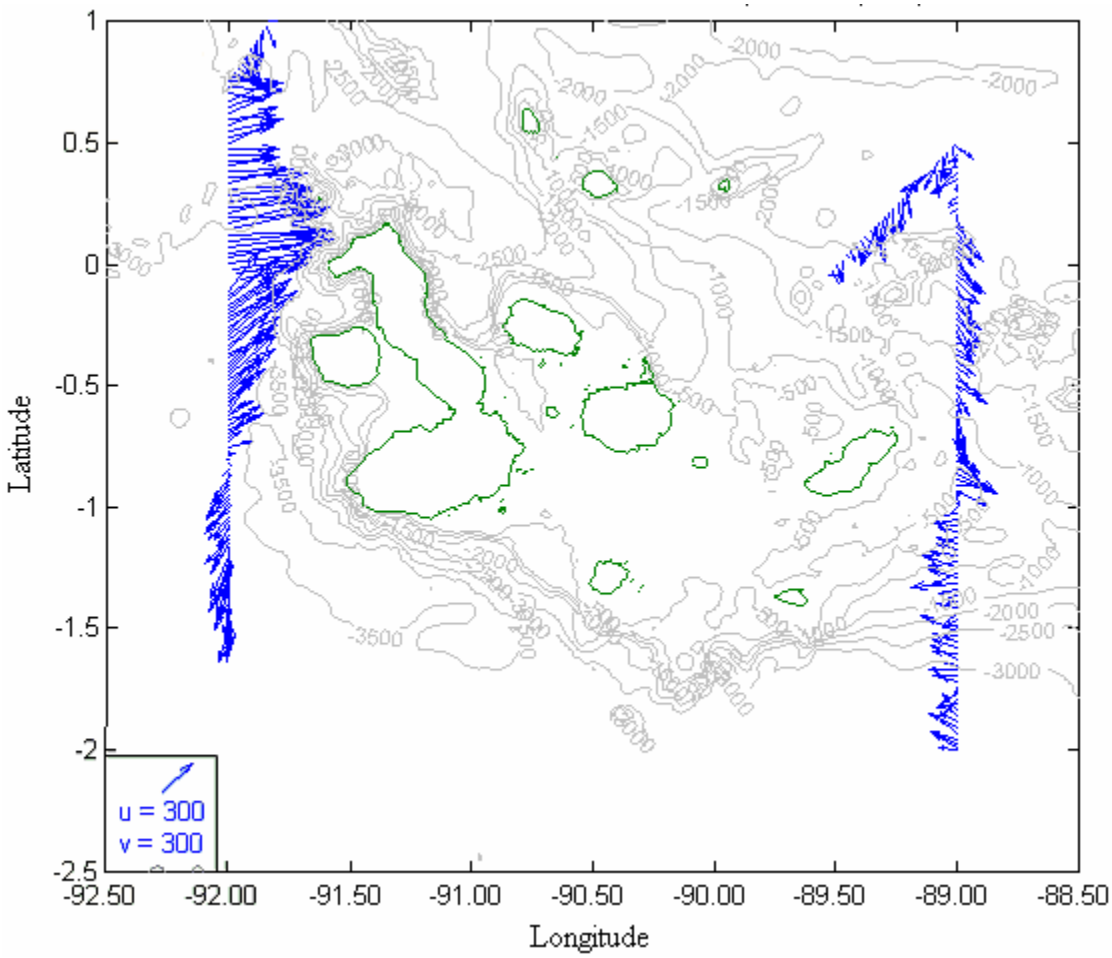

D. Velocity vectors at 76 m.

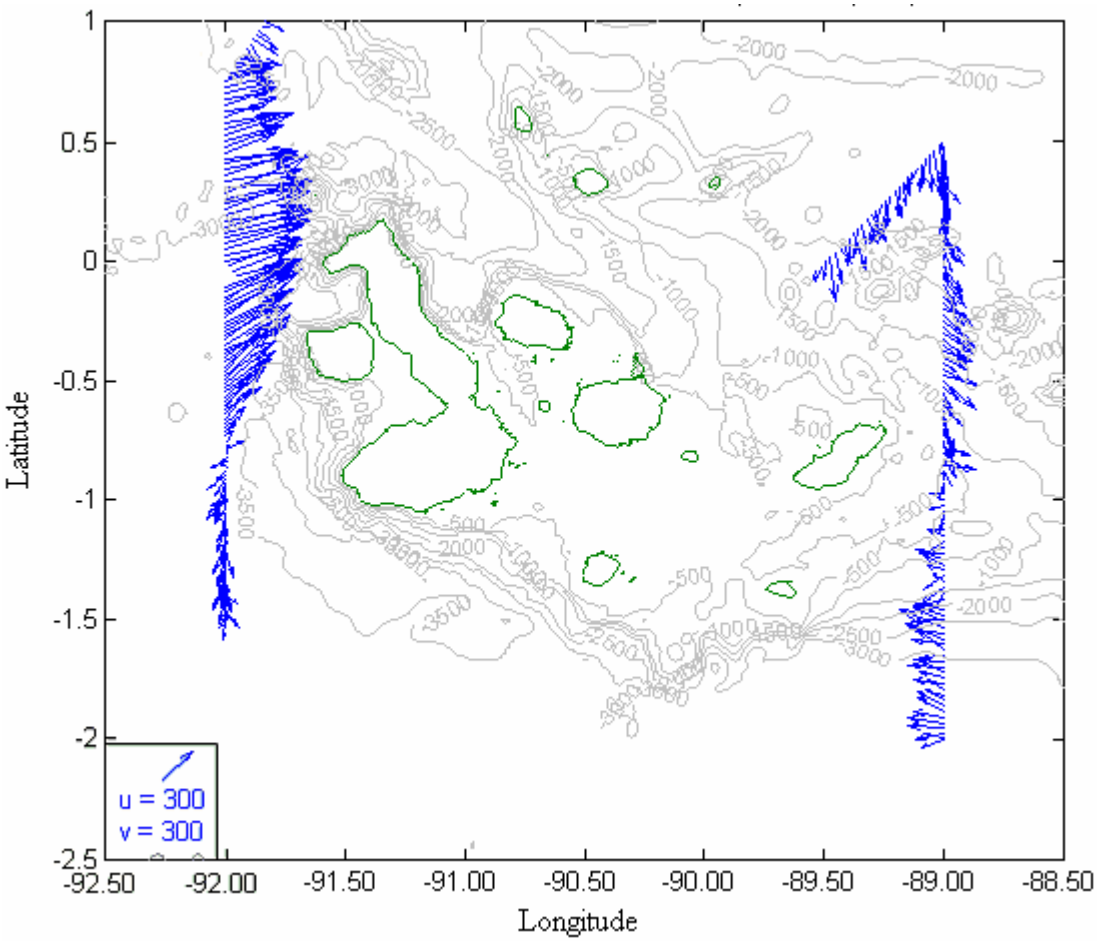

E. Velocity vectors at 100 m.

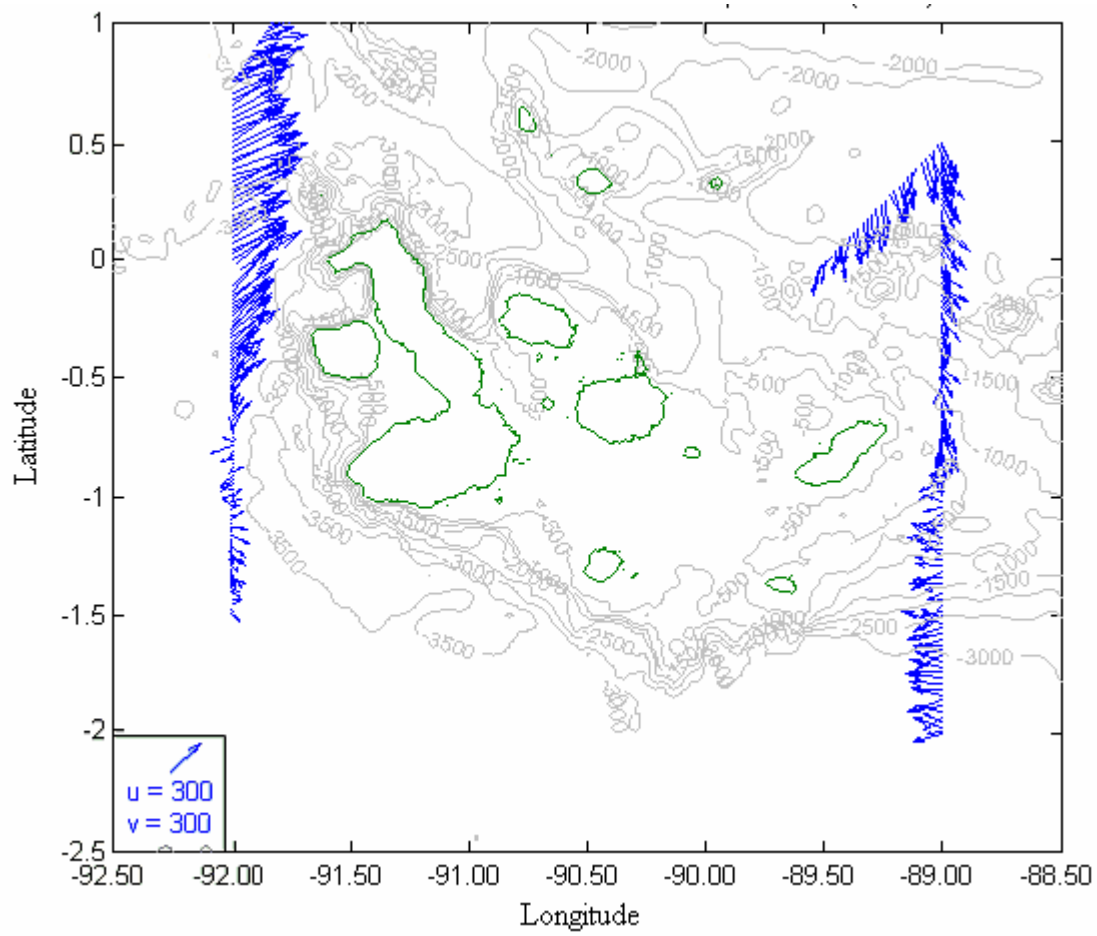

Figure 5.

A. East-West velocity

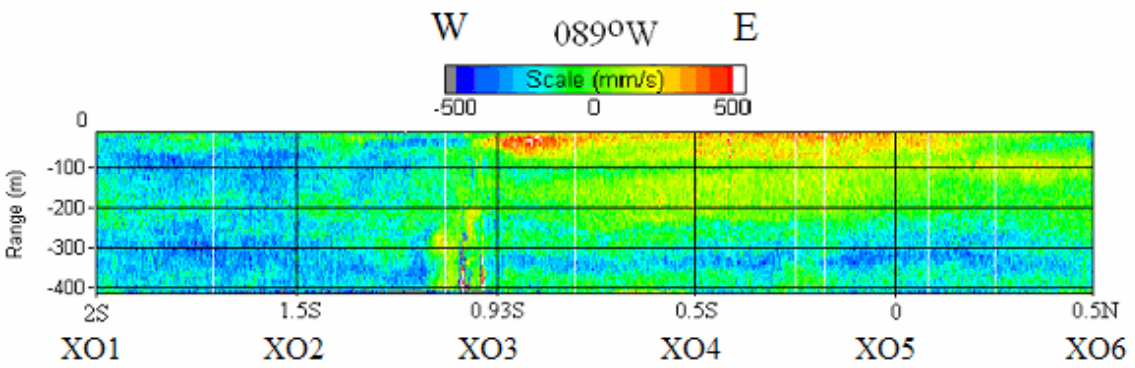

B. North-South velocity

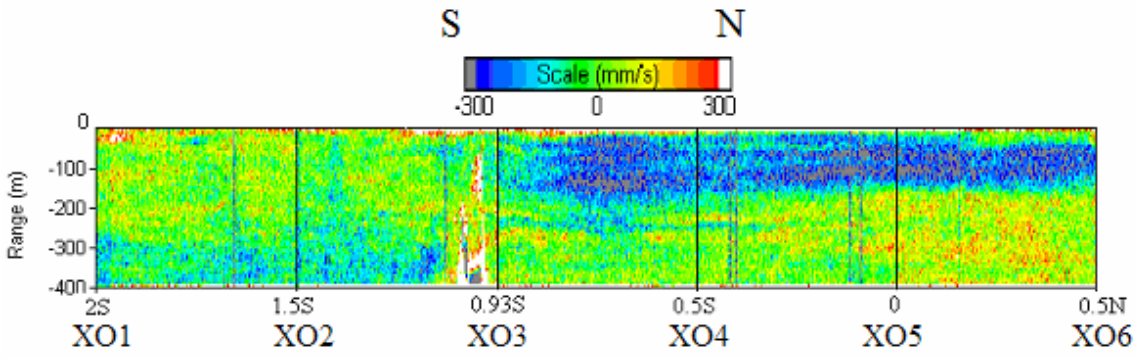

Figure 6.
A.

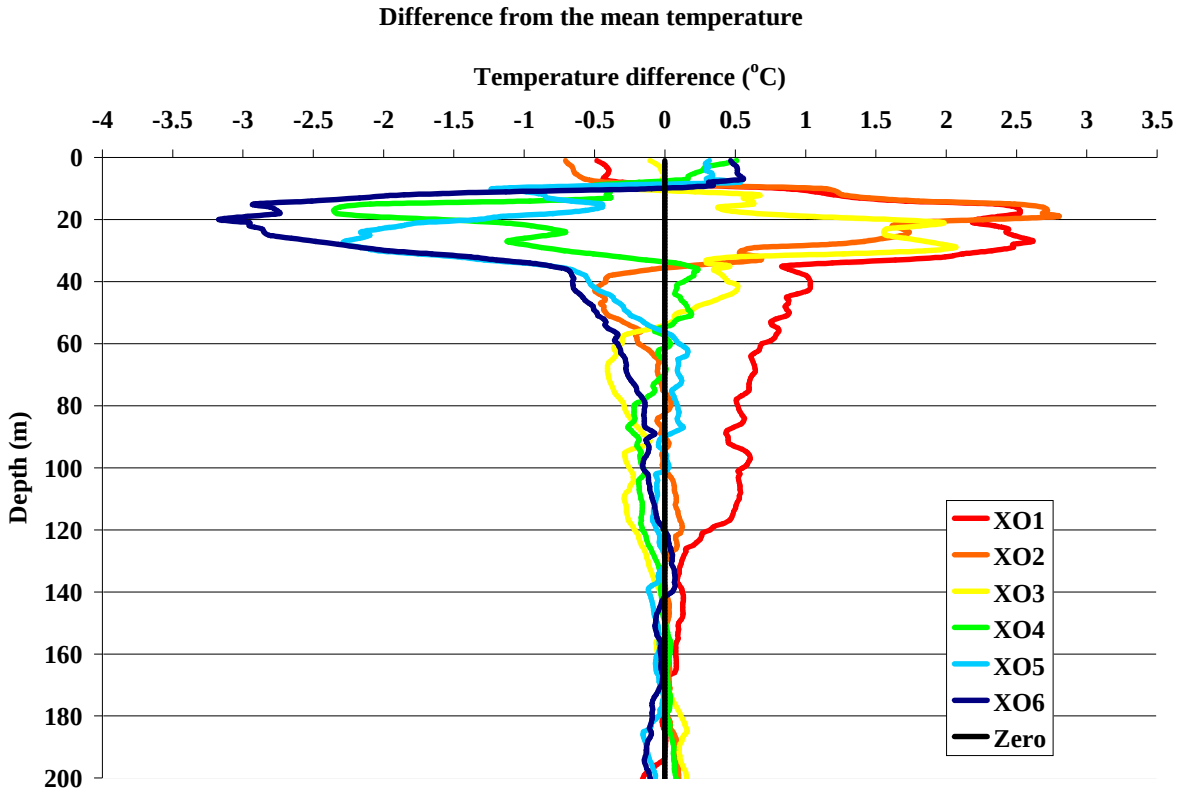
Difference from the mean temperature
Temperature difference (°C)
-4
-3.5
-3
-2.5
-2
-1.5
-1
-0.5
0
0.5
1
1.5
2
2.5
3
3.5
Depth (m)
0
20
40
60
80
100
120
140
160
180
200
XO1
XO2
XO3
XO4
XO5
XO6
Zero

B.

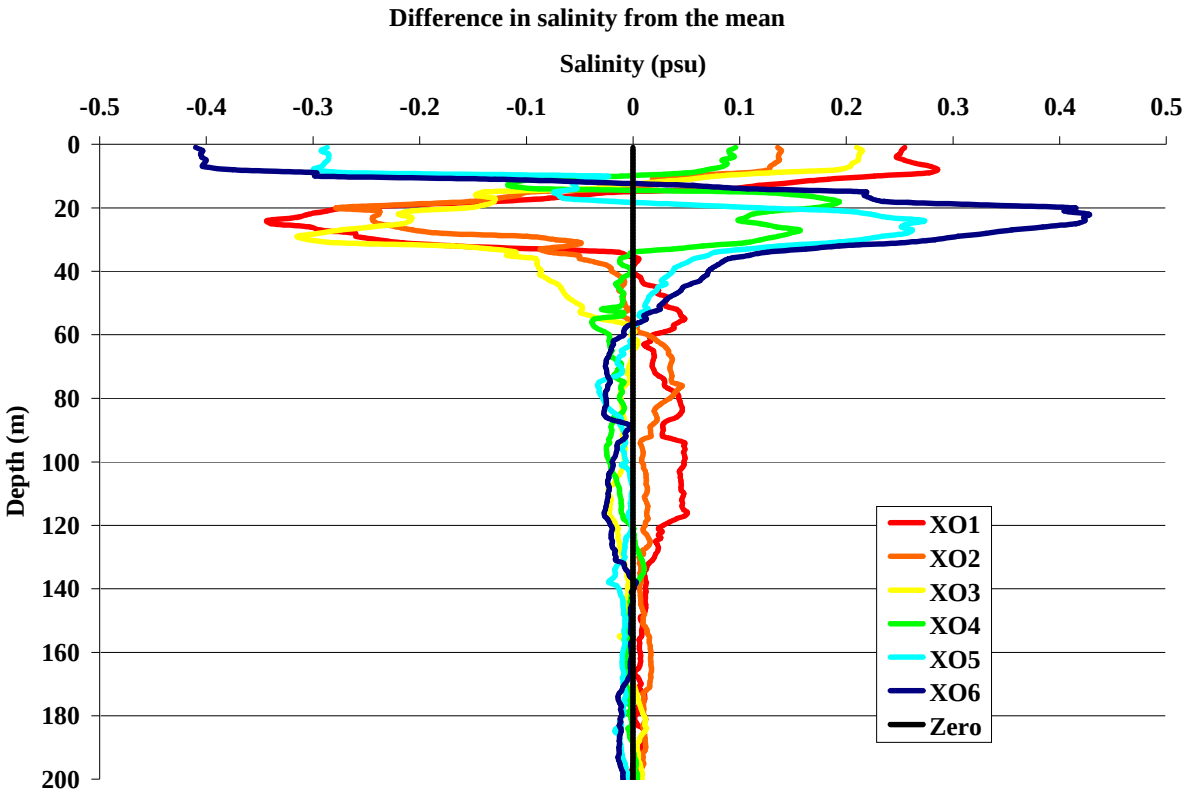
Difference in salinity from the mean
Salinity (psu)
-0.5
-0.4
-0.3
-0.2
-0.1
0
0.1
0.2
0.3
0.4
0.5
Depth (m)
0
20
40
60
80
100
120
140
160
180
200
XO1
XO2
XO3
XO4
XO5
XO6
Zero

C.

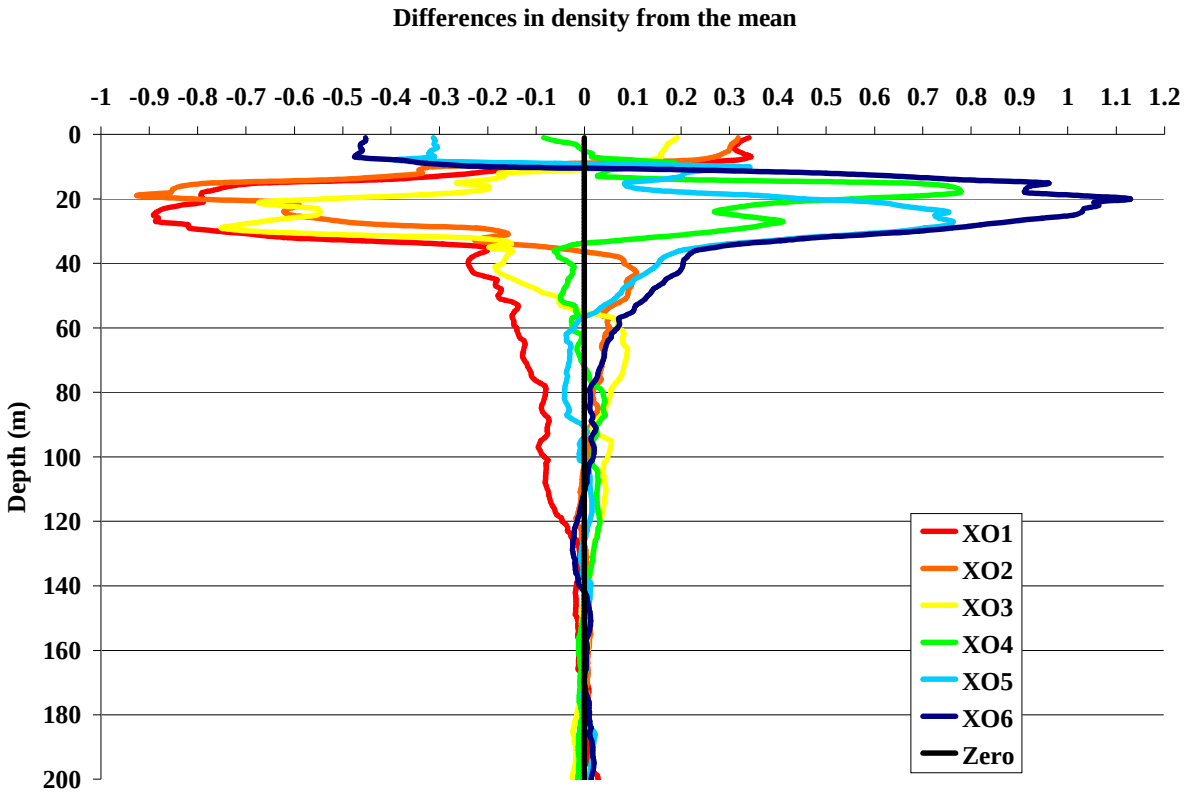
Differences in density from the mean
-1 -0.9 -0.8 -0.7 -0.6 -0.5 -0.4 -0.3 -0.2 -0.1 0 0.1 0.2 0.3 0.4 0.5 0.6 0.7 0.8 0.9 1 1.1 1.2
Depth (m)
0 20 40 60 80 100 120 140 160 180 200
XO1
XO2
XO3
XO4
XO5
XO6
Zero

Figure 7.

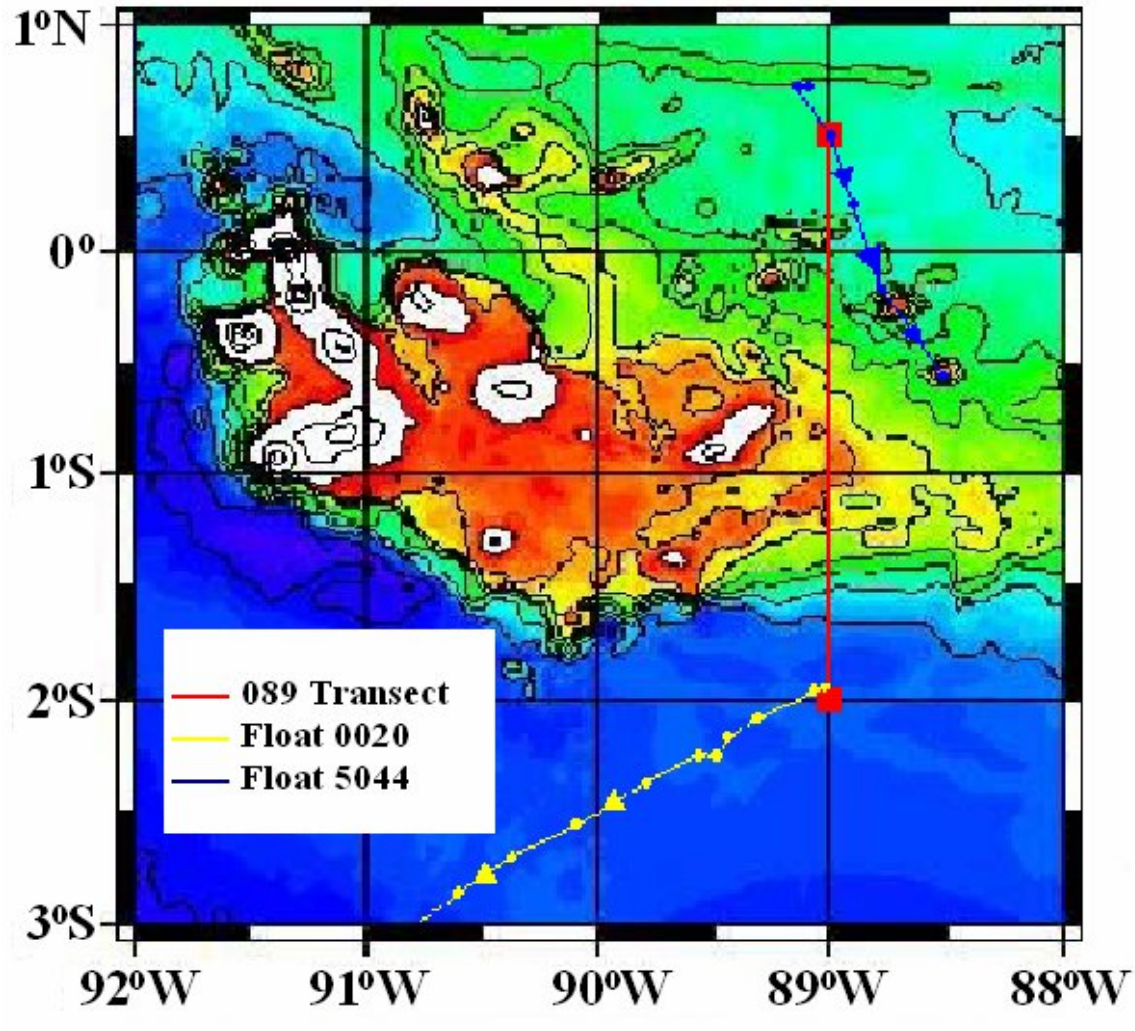
1ºN
0º
1ºS
2ºS
3ºS
92ºW
91ºW
90ºW
89ºW
88ºW
089 Transect
Float 0020
Float 5044

Figure 8.

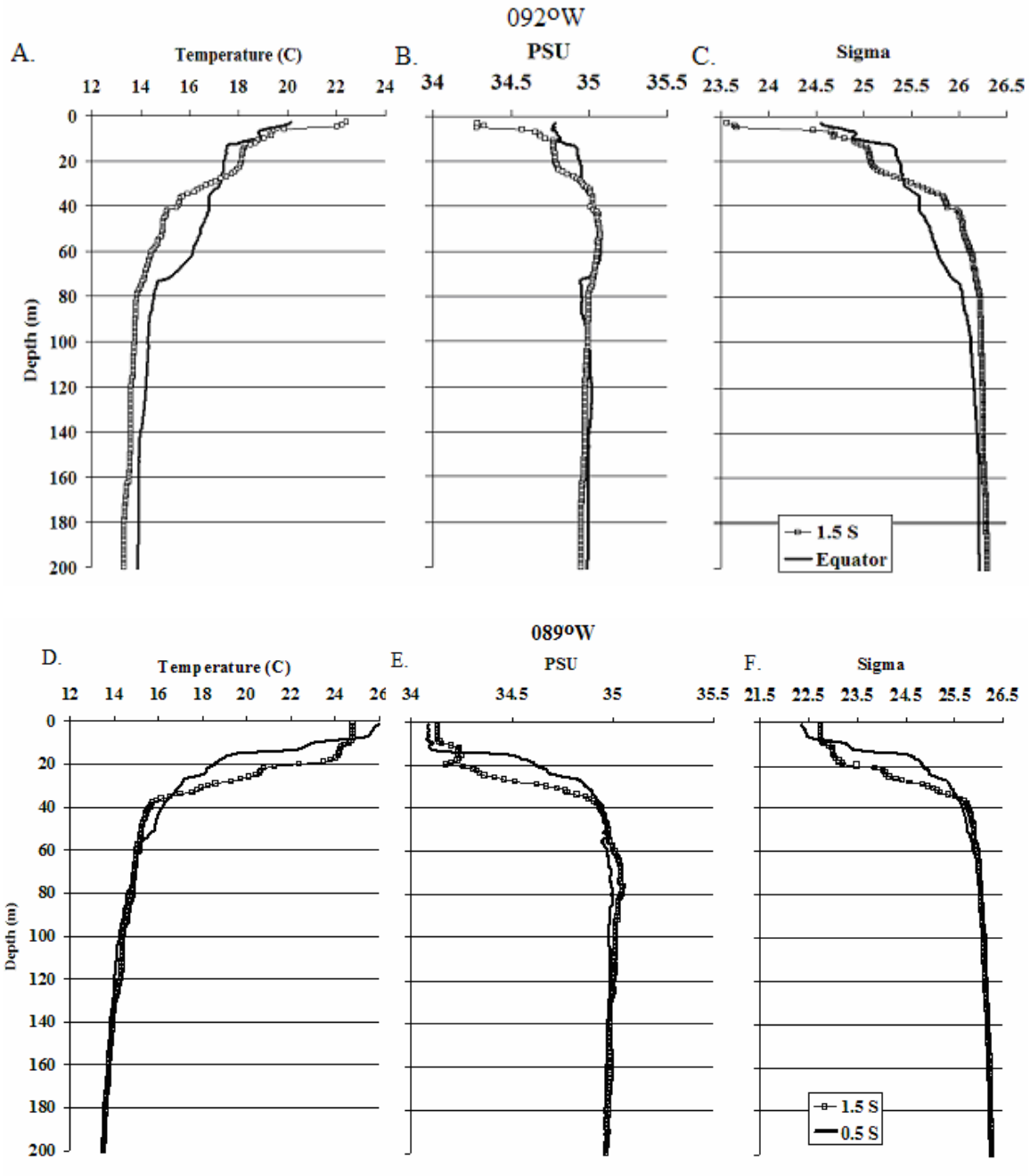
092°W
A.
Temperature (C)
12 14 16 18 20 22 24
B.
PSU
34 34.5 35 35.5
C.
Sigma
23.5 24 24.5 25 25.5 26 26.5
Depth (m)
0 20 40 60 80 100 120 140 160 180 200
1.5 S
Equator
089°W
D.
Temperature (C)
12 14 16 18 20 22 24 26
E.
PSU
34 34.5 35 35.5
F.
Sigma
21.5 22.5 23.5 24.5 25.5 26.5
Depth (m)
0 20 40 60 80 100 120 140 160 180 200
1.5 S
0.5 S